



## Characteristics of the citrate-based zinc–polyaniline secondary cell with supercapattery behaviour

BRANIMIR N. GRGUR<sup>1\*</sup>, MILICA M. GVOZDENOVIC<sup>1#</sup>, BRANIMIR Z. JUGOVIĆ<sup>2</sup>  
and TOMISLAV Lj. TRIŠOVIĆ<sup>2</sup>

<sup>1</sup>Faculty of Technology and Metallurgy, University of Belgrade, Karnegijeva 4, Belgrade,  
Serbia and <sup>2</sup>Institute of Technical Science, Serbian Academy of Science and Arts,

Knez Mihailova 35, 11000 Belgrade, Serbia

(Received 9 July, accepted 19 July 2019)

**Abstract:** The electrochemical characteristics of zinc–polyaniline (PANI) secondary cell in the electrolyte containing 0.8 M Na citrate, 0.3 M NH<sub>4</sub>Cl and 0.3 M ZnCl<sub>2</sub> is investigated. Based on the measurements of potentials and voltage of the cell during charge/discharge for the currents in the range of 18 to 45 mA, the specific electrode capacity of 85 to 55 mA h g<sup>-1</sup>, the specific energy of 60–40 mW h g<sup>-1</sup> and the specific power of 150–350 mW g<sup>-1</sup>, is determined.

**Keywords:** polyaniline; zinc; batteries; pseudocapacitors; citrates.

### INTRODUCTION

Polyaniline (PANI) as a conducting polymer, which due to the practically reversible doping–dedoping reaction with anions from the electrolyte represent the class of organic semiconductors, could be used as an electrode material for the secondary electrochemical power source, as a pseudocapacitive like material. The idea that polyaniline could be used as an electrode material in electrochemical power sources is suggested by Nobel laureate MacDiarmid *et al.*<sup>1</sup> Polyaniline has some potential advantages considering some other classical systems, like small mass, inexpensive synthesis, ecological acceptability, fast redox behaviour, *etc.*<sup>2</sup> In recent years, polyaniline is investigated as a supercapacitive material.<sup>3</sup> It is also concluded that a cell based on polyaniline and some classical battery electrode materials behaves as a “supercapattery” (supercapacitor+battery) system.<sup>4,5</sup> Batteries have high specific energy ~100 Wh kg<sup>-1</sup> but low specific power ~50 W kg<sup>-1</sup>, while supercapacitors (SCs) have high specific power, in the range of 0.1 to 10 kW kg<sup>-1</sup> but low specific energy, 1 to 10 Wh kg<sup>-1</sup>.<sup>6</sup> Combining the pseudocapacitive and battery type electrode in a supercapattery can bridge the gap

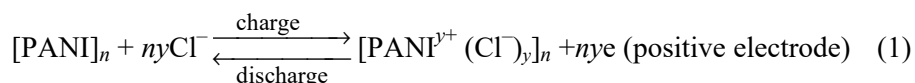
\* Corresponding author: E-mail: BNGrugur@tmf.bg.ac.rs

# Serbian Chemical Society member.

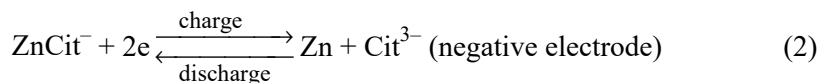
<https://doi.org/10.2298/JSC190709077G>

between the battery and SCs, as well as offer means of achieving both high energy and high power density for long cycles.<sup>7</sup>

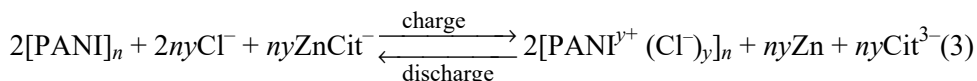
In our previous study<sup>8</sup>, investigating the half-cell electrode reactions, the optimum electrolyte composition of 0.8 M sodium citrate, 0.3 M ammonium chloride, and 0.3 M zinc chloride is suggested for the Zn|PANI secondary electrochemical cell. Such electrochemical system is based on the following half-cell reactions:



where  $y$  is doping degree (number of anions per polymer units), and:



The reactions during charge/discharge of the complete cell will be as follows:



Based on these results, the aim of this work is the investigation of the real Zn|PANI secondary cell characteristics in the suggested electrolyte.

## EXPERIMENTAL

The electrodes, 1 mm pure zinc plate ( $3.6 \text{ cm} \times 5 \text{ cm}$ ,  $S = 18 \text{ cm}^2$ ) and 3-mm thick graphite ( $3.6 \text{ cm} \times 5 \text{ cm}$ ,  $S = 18 \text{ cm}^2$ ) plate, were used in all experiments. Back sides of the electrodes were isolated using glued tin (0.5 mm) Plexiglas cover. Before each experiment, the electrodes were mechanically polished with fine emery papers (2/0, 3/0 and 4/0, respectively). After mechanical polishing, the traces of impurities were removed from the electrode surface in an ultrasonic bath filled with ethanol for 5 min.

Polyaniline electrode was electrochemically polymerized on graphite electrode from 1 M hydrochloric acid solution with the addition of 0.25 M aniline monomer (p.a. Merck, previously distilled under argon atmosphere), at a constant current of 36 mA ( $2 \text{ mA cm}^{-2}$ ) during 5000 s. After polymerization, the electrode was washed with bi-distilled water and transferred into the second electrochemical cell for further investigations. One sample was only washed a few times with bi-distilled water after polymerization, then dried in the oven ( $90^\circ\text{C}$ ) during the night, and PANI mass is determined as a mass difference.

The electrolyte containing 0.8 M sodium citrate, 0.3 M ammonium chloride, and 0.3 M zinc chloride was prepared from p.a. grade chemicals (Merck) and bi-distilled water. pH of the electrolyte, ~5, is adjusted by 2 M sodium hydroxide and 1 M citric acid. The pH was chosen to be in agreement with the zinc corrosion rate and PANI activity that decreased at higher pH.

For all experiments, only one compartment prismatic Plexiglas cell, with dimension  $10 \text{ cm} \times 3.6 \text{ cm} \times 3 \text{ cm}$ , with an electrode gap of 10 mm is used. The saturated calomel electrode (SCE),  $E_r = 0.244 \text{ V}$  vs. SHE, placed between PANI and the zinc electrode, was used as a reference electrode. All potentials are referred to SCE scale. The electrochemical measurements

were carried out using Gamry PC3 potentiostat/galvanostat controlled by computer *via* an interface. The voltage of the cell was measured and collected using ISO-TECH IDM 73 multimeter connected to the computer *via* RS 232 interface.

## RESULTS AND DISCUSSION

### *Synthesis and characterization of the PANI and zinc electrode*

Fig. 1 shows the galvanostatic curve of the aniline polymerization from the solution containing 1 M HCl and 0.25 M aniline monomer on the graphite electrode at the current of 36 mA ( $2 \text{ mA cm}^{-2}$ ) during 5000 s with the polymerization charge ( $Q_p$ ) of 50 mA h. The polymerization starts at the potential of  $\sim 0.7 \text{ V}$  and proceeds in the potential range between 0.65 and 0.55 V. After the polymerization, the electrode is washed with bi-distilled water and transferred into the electrochemical cell with chloride/citrate electrolyte for further investigations.

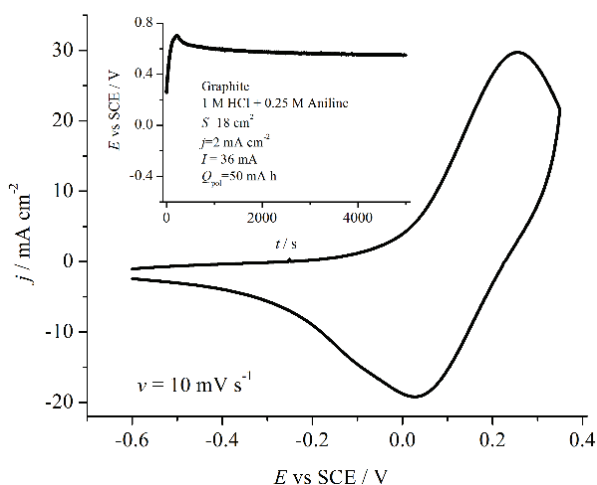


Fig. 1. Cyclic voltammogram of PANI electrode in the electrolyte containing 0.8 M sodium citrate, 0.3 M ammonium chloride and 0.3 M zinc chloride. Inset: galvanostatic curve for aniline polymerization in the solution containing 1 M HCl and 0.25 M aniline on a graphite electrode.

In Fig. 1 the cyclic voltammogram of the PANI electrode in the chloride/citrate based electrolyte is also shown. Doping of the PANI occurred in the potential range of  $-0.1$  to  $0.35 \text{ V}$ , while dedoping in the potential range of  $0.25$  to  $-0.02 \text{ V}$ . The maximum peak for doping is positioned at  $0.26 \text{ V}$ , and for dedoping  $-0.02 \text{ V}$ . The citrates are not considered as a doping anion of PANI electrode, because it is suggested that at the less positive potentials doping proceeds with chloride and at the more positive potentials ( $>0.35 \text{ V}$ ) with citrates, where faster degradation occur.<sup>8,9</sup>

After the cyclic voltammetry experiments, the electrode is conditioned at the potential of  $-0.6 \text{ V}$  for 180 s to be completely dedoped, and two initial cycles of

charge/discharge are applied with the current density of 36 mA to obtain reproducibility. Fig. 2 shows the dependence of the PANI electrode potential during doping/dedoping (charge/discharge) at different currents. The potentials are limited to 0.35 V for charge and to -0.4 V for discharge. Charge of the discharged PANI electrode starts at the potential of  $\sim$ -0.17 V. Depending on the applied current, the charge potential increases nonlinearly up to  $\sim$ 0.35 V. The discharge of the electrode occurs in the potential range between  $\sim$ 0.15 to -0.25 V with an average discharge potential of  $\sim$ -0.05 V, followed by the sharp decrease of the potential due to the diffusion limitations and the decreased conductivity.

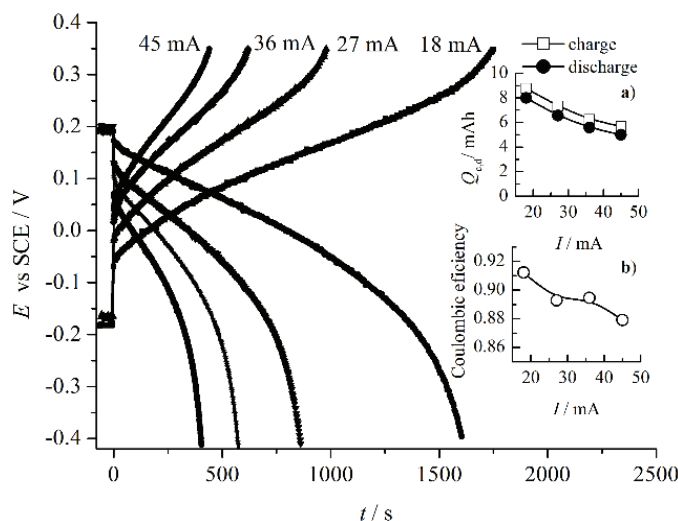


Fig. 2. Charge/discharge curves of PANI electrode for the different currents. Insets: a) Determined capacities of the charge/discharge at different currents, b) Coulombic efficiency.

Determined capacities of charge/discharge at different currents are shown in Fig. 2a. The charge/discharge capacity decreases from  $\sim$ 8 to 5 mA h with the increase of applied current. The calculated charge/discharge Coulombic efficiency, shown in Fig. 2b, is in the range of 92 to 88 %, depending on applied current.

In the separate experiment after polymerization, one PANI sample is washed only few times with bi-distilled water, dried in the oven (90 °C) during the night, and therefore PANI mass of 0.103 g was determined. The corresponding thickness of PANI electrode, assuming the density of chloride doped PANI of 1.38 g cm<sup>-3</sup> is estimated to be  $\sim$ 41  $\mu$ m.<sup>10</sup> For the determined PANI mass, and the specific charge/discharge capacity in the range of 78 to 48 mAh g<sup>-1</sup>, are estimated.

The polarization curve of a solid zinc electrode in the electrolyte containing 0.8 M Na citrate, 0.3 M NH<sub>4</sub>Cl and 0.3 M ZnCl<sub>2</sub> is shown in Fig. 3.

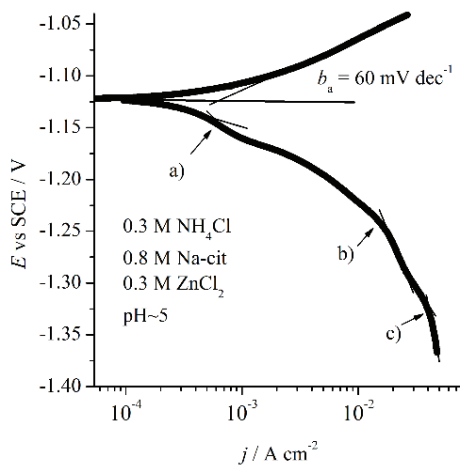
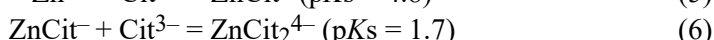
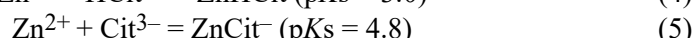


Fig. 3. IR corrected polarization curve of the zinc electrode in the electrolyte containing 0.8 M Na citrate, 0.3 M  $\text{NH}_4\text{Cl}$  and 0.3 M  $\text{ZnCl}_2$ .

Anodic part of the polarization curve is characterized with the single Tafel slope of  $\sim 60 \text{ mV dec}^{-1}$ , up to the current densities of  $30 \text{ mA cm}^{-2}$ . The cathodic part has few not well-defined waves, marked with a)-c), which could be connected with the limiting currents. Hence, the value of the cathodic Tafel line in this electrolyte cannot be determined. At  $\text{pH} \sim 5$  in the presence of citrate in solution, zinc ion forms different types of complexes, with suggested main species<sup>11</sup>:



Due to the values of the stability constants, it could be suggested that the main species in the solution is  $\text{ZnCit}^-$ , the concentration of  $\text{ZnHCit}$  is considerably smaller, while the concentrations of  $\text{ZnCit}_2^{4-}$  and free zinc ions are rather low. Therefore, the few waves in the cathodic part of the polarization curve (Fig. 3) could be assigned to the reduction of different species from the solution.

#### *Characteristics of the Zn|PANI cell*

During charge/discharge, simultaneously with PANI electrode potentials at different currents shown in Fig. 2, the voltage of the cell is measured and results are shown in Fig. 4. Depending on the applied currents, the charge of the cell occurred in the voltage range of 0.9 and 1.9 V. As can be seen, the charging voltage limit ( $U_{l,c}$ ) increase by increasing the applied current. Because, the charging potential limit for PANI electrodes is set constant (0.35 V), the nonlinear increase of the charging voltage could be mainly connected to the zinc deposition reaction and by the influence of the electrolyte ohmic drops. After the charge, the open circuit voltage ( $U_0$ ) of  $\sim 1.35 \text{ V}$  is determined. The discharge of the cell,

depending on current, occurred in the voltage range between 1.2–1 V to ~0.5 V. The average useful voltage is ~0.9 V.

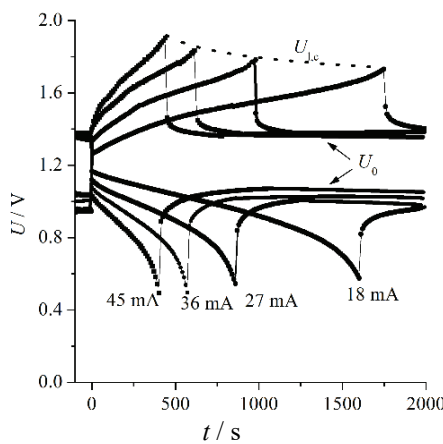


Fig. 4. The voltage of the PANI|Zn cell for different currents.  $U_{l,c}$  – limiting charging voltage,  $U_0$  – open circuit voltage.

According to the results presented in Fig. 4, it is possible to calculate the specific discharge capacity ( $q_s$ ), energy ( $w_s$ ) and power ( $P_s$ ) based on the electrode mass. Because the mass of the as-synthesized PANI is known (~0.103 g) from the times for discharge at specific currents (Fig. 4), it is possible to calculate the mass of the zinc involved in the discharge (d) reaction using Faraday law:

$$m_d(\text{Zn}) = I_d t_d \frac{M(\text{Zn})}{2 \times 26.8} \eta_{I,d}(\text{Zn}) \quad (6)$$

where  $I_d$  represents the current,  $t_d$  is the time,  $M(\text{Zn})$  is the atomic mass of the zinc, 26.8 is Faraday constant, and  $\eta_{I,d}(\text{Zn})$  is the determined current efficiency for zinc deposition.<sup>8</sup> The calculated values are summarized and given in Table I. Knowing the involved mass of the zinc during the discharge, the specific current:

$$I_s = \frac{I_d}{m(\text{PANI}) + m(\text{Zn})} \quad (7)$$

can be also estimated in the range of ~160 to 400 mA g<sup>-1</sup> based on the active mass.

TABLE I. The calculated values for zinc mass during discharge and the values of the specific currents ( $m(\text{PANI}) = 0.103$  g)

$I_d$ / mA	$Q_d$ / mA h	$m_d(\text{Zn})$ / mg	$I_s$ / mA g <sup>-1</sup>
18	8.0	9.8	160
27	6.6	8.0	243
36	5.6	6.8	350
45	4.8	5.9	413

The specific capacity of the cell for discharge (for  $I_d$  in mA and  $t_d$  in s) can be calculated using:

$$q_s = \frac{I_d t_d}{3600 [m_d(\text{Zn}) + m(\text{PANI})]} = \frac{Q_d}{3600 m_d} \quad (8)$$

the specific energy during discharge, using:

$$w_d = \frac{I_d}{3600 m_d} \int_0^t U_d dt \quad (9)$$

and the specific power during discharge from:

$$P_d = \frac{w_d}{\Delta t} = \frac{I_d 3600}{m_d \Delta t} \int_0^t U_d dt \quad (10)$$

The calculated values are shown in Fig. 5. An average specific capacity, based on the active mass in the cell is in the range of 75 to 50 mA h g<sup>-1</sup>, the discharge specific energy is in the range of 67 to 37 mW h g<sup>-1</sup>, while the discharge specific power is in the range of 155 to 350 mW g<sup>-1</sup>, depending on the applied current. Therefore, such a system has a reasonable specific energy in the range of classical battery systems and an increased specific power. It should be mentioned that the similar characteristics are obtained for the zinc-polypyrrole system in the ammonium chloride electrolyte, which shows the specific power of 325 mW g<sup>-1</sup> at the current of 380 mA g<sup>-1</sup>.<sup>12</sup>

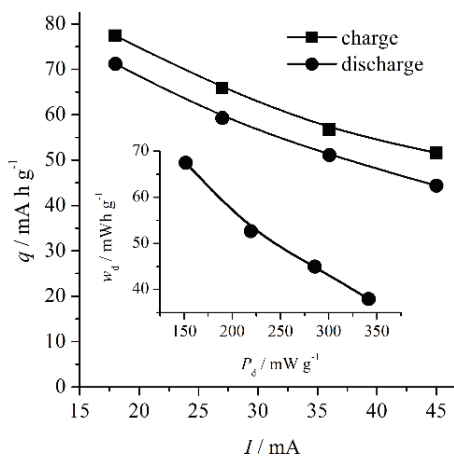


Fig. 5. Dependence of specific charge/discharge capacity of the cell on current. Inset: Dependence of the discharge specific energy on specific power.

The characteristics of the cell during cyclization are investigated applying the current density of 36 mA during 25 cycles, and the results are shown in Fig. 6. Practically no deterioration of the characteristics is observed.

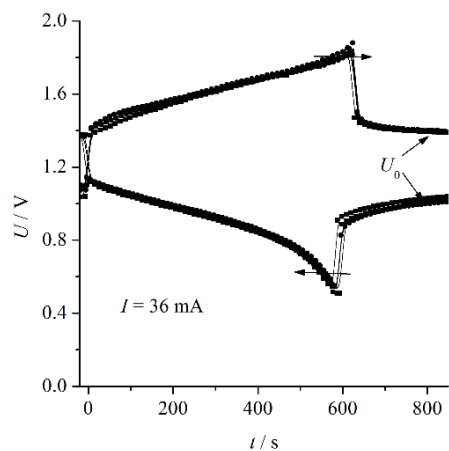


Fig. 6. Charge/discharge characteristic of the cell for 1<sup>st</sup>, 10<sup>th</sup>, 15<sup>th</sup> and 25<sup>th</sup> cycle.

The self-discharge rate is determined for the system charged/discharged with a current of 18 mA before and after 120 h, as shown in Fig 7. During the time, the open circuit voltage of the charged cell decrease from the initial value of  $\sim 1.4$  V to  $\sim 1.33$  V, as shown in the inset of Fig. 7.

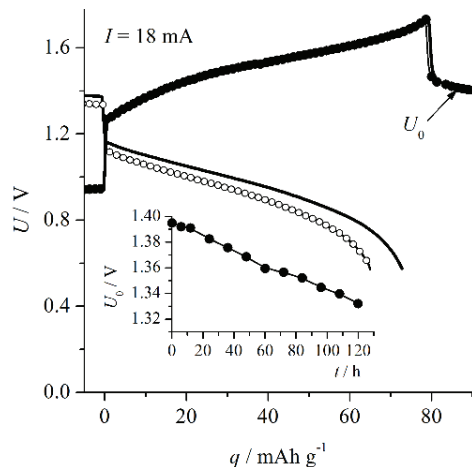


Fig. 7. Determination of self-discharge rate of Zn|PANI cell. First charge/discharge (—) and discharge after 120 h (○). Inset: Dependence of the open circuit voltage of the charged cell over time.

The discharge capacity of the cell was  $\sim 10\%$  smaller than the initial one, giving an average self-discharge rate of  $2\%$  per day. Because, the anode is the solid zinc with the relatively stable open circuit potential, the self-discharge could be connected with the behaviour of PANI electrode. As elaborated by Rahmanifar *et al.*<sup>13</sup>, hydroquinone is one of the main degradation products in the solid PANI film, which further interacts with the oxidized PANI form, and producing the self dedoping or the self-discharge of the cell.

## CONCLUSION

Based on the presented results, the following conclusions of the investigated systems could be drawn. Zn|PANI secondary cell can be successfully charged in the voltage range of 1.2 to 1.9 V, with a specific current of 160 to  $\sim$ 450 mA g $^{-1}$ . Under these conditions, the specific electrode capacity of 85 to 55 mA h g $^{-1}$ , the specific energy of 60–40 mW h g $^{-1}$  and the specific power of 150–350 mW g $^{-1}$  were determined. Due to the increased specific power in comparison with classical battery systems, such cell could be classified as a supercappattery.

*Acknowledgement.* The research is supported by the Ministry of Education, Science and Technological Development of the Republic of Serbia, under the research project “Electrochemical synthesis and characterization of nanostructured functional materials for applications in new technologies” No. ON172046.

## ИЗВОД

## КАРАКТЕРИСТИКЕ ЦИНК–ПОЛИАНИЛИН СЕКУНДАРНЕ ЋЕЛИЈЕ НА БАЗИ ЦИТРАТНИХ РАСТВОРА СА СУПЕРКАПАБАТЕРИЈСКИМ ПОНАШАЊЕМ

БРАНИМИР Н. ГРГУР<sup>1</sup>, МИЛИЦА М. ГВОЗДЕНОВИЋ<sup>1</sup>, БРАНИМИР З. ЈУГОВИЋ<sup>2</sup> И ТОМИСЛАВ Љ. ТРИШОВИЋ<sup>2</sup>

<sup>1</sup>Технолошко–мештаришки факултет у Београду, Универзитет у Београду, Карнеجيјева 4, Београд и <sup>2</sup>Институт за техничких наука, Српске академије наука и уметности, Кнез Михаилова 35, 11000 Београд

Испитане су електрохемијске карактеристике секундарне ћелије цинк–полианилин (PANI) у електролиту који садржи 0,8 M Na-цитрат, 0,3 M NH<sub>4</sub>Cl и 0,3 M ZnCl<sub>2</sub>. На основу мерења потенцијала и напона ћелије за време пуњења/пражњења у опсегу струја од 18 до 45 mA, одређени су специфични капацитети од 85 до 55 mA h g $^{-1}$ , специфична енергија 60–40 mW h g $^{-1}$  и специфична снага од 150–350 mW g $^{-1}$ .

(Примљено 9. јула, прихваћено 19. јула 2019)

## REFERENCES

1. A. G. MacDiarmid, J. C. Chiang, M. Halpern, W. S. Huang, J. R. Krawczyk, R. J. Mammone, S. L. Mu, N. L. D. Somasiri and W. Wu, *Polym. Prep. Am. Chem. Soc. Div. Polym. Chem.* **252** (1984) 248
2. P. Novák, K. Müller, K. S. V. Santhanam, O. Haas, *Chem Rev.* **97** (1997) 207 (<https://doi.org/10.1021/cr941181o>)
3. A. Eftekhari, L. Li, Y. Yang, *J. Power Sources* **347** (2017) 86 (<https://doi.org/10.1016/j.jpowsour.2017.02.054>)
4. A. A. Alguail, A. H. Al-Eggiely, B. N. Grgur, *J. Saudi Chem. Soc.* **21** (2017) 575 (<https://doi.org/10.1016/j.jscs.2017.01.002>)
5. L. Yu, G. Z. Chen, *J. Power Source* **326** (2016) 604 (<https://doi.org/10.1016/j.jpowsour.2016.04.095>)
6. M. Winter, R. J. Brodd, *Chem. Rev.* **104** (2004) 4245 (<https://doi.org/10.1021/cr020730k>)
7. A. A. Alguail, A. H. Al-Eggiely, M. M. Gvozdenović, B. Z. Jugović, B. N. Grgur, *J. Power Sources* **313** (2016) 240 (<https://doi.org/10.1016/j.jpowsour.2016.02.081>)
8. B. Jugović, M. Gvozdenović, J. Stevanović, T. Trišović, B. Grgur, *J. Appl. Electrochem.* **39** (2009) 2521 (<https://doi.org/10.1007/s10800-009-9946-7>)
9. B. Z. Jugović, T. Lj. Trišović, J. S. Stevanović, M. D. Maksimović, B. N. Grgur, *Electrochim. Acta* **51** (2006) 6268. (<https://doi.org/10.1007/s10800-009-9946-7>)

10. J. Stejskal, D. Hlavatá, P. Holler, M. Trchová, J. Prokeš, I. Sapurina. *Polym Int.* **53** (2004) 294 (<https://doi.org/10.1002/pi.1406>)
11. G. Berthon, P. M. May, D. R. Williams, *J. Chem. Soc., Dalton Trans.* **11** (1978) 1433 (<https://doi.org/10.1039/DT9780001433>)
12. B. N. Grgur, M. Janačković, B. Z. Jugović, M. M. Gvozdenovića, *Mater. Sci. Eng., B-Adv.* **243** (2019) 175 (<https://doi.org/10.1016/j.mseb.2019.04.013>)
13. M. S. Rahmanifar, M. F. Mousavi, M. Shamsipur, H. Heli, *Synth. Met.* **155** (2005) 480 (<https://doi.org/10.1016/j.synthmet.2005.06.009>).